A stochastic flamelet progress-variable approach for numerical simulations of high-speed turbulent combustion under chemical-kinetic uncertainties

By J. Urzay, N. Kseib, F. Palacios, J. Larsson AND G. Iaccarino

1. Motivation and objectives

In this study, a flamelet-based framework is proposed for quantifying the uncertainties induced by chemical-kinetic rates on the aerothermochemical field in numerical simulations of high-speed turbulent combustion. For this purpose, this report is divided into the following sections. In Section 2, a short background on flamelet physics is provided. In Section 3, the RANS formulation of the outer problem is summarized. In Section 4 the flamelet progress-variable approach (FPVA) for modeling turbulent combustion (Pierce & Moin 2004) is extended to treat uncertainties in chemical kinetics. In Section 5, a strategy for propagating input uncertainties in the main aerothermochemical variables is proposed. Section 6 is focused on a short assessment of the potential effects of chemical-kinetic uncertainties in the hydrogen-fueled Hyshot-II SCRAMJET engine. Finally, conclusions are drawn in Section 7. This work is founded upon another article that appears in this same volume (Urzay *et al.* 2012) for quantifying uncertainties in chemical-kinetic rates.

2. Background

It is well known that, in addition to the closures needed for turbulent fluxes, the chemical-source terms need closure in turbulent reacting flows when the filtering or averaging operators are applied to the conservation equations; the reasons for this are that combustion typically occurs in subgrid scales that are filtered out (in the case of LES), and that ensemble or time-averaging of the combustion process leads to thickened flames where chemical reaction takes place in the mean (in the case of RANS). In both cases, it is widely accepted that the averaged or filtered chemical-production term is not quite given by eq. (2.1) in Urzay *et al.* (2012) if directly written in terms of the averaged or filtered aerothermochemical variables.

Among many other turbulent-combustion models used for attaining closure of the chemical-production terms, the steady non-premixed flamelet model (Peters 2000) is based on the belief that a complex turbulent diffusion flame can be decomposed on elementary flames which are subject to a local stagnation-point strain field in the microscale ℓ_m -which is of the same order as the Batchelor length-, as depicted in Figure 1(a). The resulting counterflow diffusion flame undergoes bifurcations that were first described in a seminal paper by Liñán in the limit of large activation energies (Liñán 1974), and which served as the fundamental pillar in later developments in flamelet models (Peters 1983). In particular, Liñán found that multiple solutions occur for the same value of the

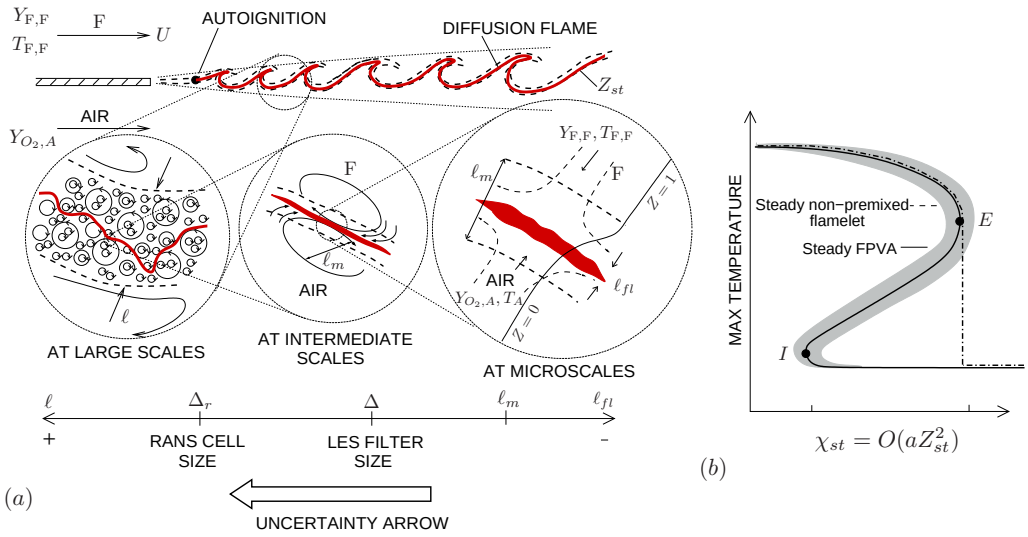

FIGURE 1. (a) Instantaneous flamelet concept for a high-speed fuel-air mixing layer downstream from a splitter plate. (b) Sketch of Liñán's S-curve for a counterflow diffusion flame (Liñán 1974), with the grey area representing the zone where the influences of chemical-kinetic rate uncertainties are the largest.

strain rate a -a quantity of the same order as the inverse of the microscale time ℓ_m^2/D_F, with D_F being the fuel diffusivity-, as depicted in Figure 1(b). In particular, according to Liñán's analysis, an upper branch describes the limit of vigorously burning flames, in which the chemical time scale is much shorter than the strain time, and reactants become depleted very quickly as they flow through the mixing layer. Similarly, a lower branch describes the chemically-frozen mixing of fuel and oxidizer, during which the chemical time scale is much longer than the diffusion time scale of the reactants across the mixing layer. The intermediate branch represents a partial-burning regime in which one of the reactants leaks abundantly through the flame. The upper and lower turning points E and I are representative of extinction and ignition, respectively. It is worth mentioning that these two turning points represent abrupt quasi-static phenomena and that no temporal dynamics, which are expected to occur near extinction or ignition, are captured in Liñán's formulation (Liñán 1974). Although Liñán's analysis is limited to single-step irreversible kinetics, the qualitative dynamics depicted in Figure 1(b) tend to persist in diffusion flames even with complex chemistry (Sánchez *et al.* 1995). However, in the case of hydrogen-air diffusion flames, the bifurcation curve sketched in Figure 1(b) may depart considerably from the S-shape in conditions of relevance for supersonic combustion, as observed in Section 6.

It should be emphasized that all flamelet models implicitly assume an asymptotically large separation of time and length scales between the combusting zones and the aerodynamically-dominated regions (Peters 2000). Such separation of scales does indeed occur in vigorously-burning flames, for which the reaction-zone thickness ℓ_{fl} is typically much smaller than the integral scale ℓ and the microscale ℓ_m, as depicted in Figure 1(a). Additionally, in the fast-chemistry limit the chemical time is much shorter than both the integral time ℓ/U and the microscale time ℓ_m^2/D_F, where U is the characteristic large-scale velocity. As a consequence, the vigorously-burning regions may be envisioned

as undergoing combustion in a locally quasi-static ambient in which the outside inertial turbulence plays little role, and for which steady non-premixed flamelets are well suited.

In the steady non-premixed flamelet model, first the microscale variables are obtained from the resolution of the counterflow diffusion flame at scales of $O(\ell_m)$, as depicted in Figure 1(a), as a function of the mixture fraction Z and the stoichiometric scalar dissipation rate χ_{st} -a quantity of order aZ_{st}^2 for hydrocarbons-. In a subsequent step, the averaged/filtered values of any flamelet variable $\Psi_{i,f}$ are computed by integrating $\widetilde{\Psi}_{i,f} = \int \Psi_{i,f} P(Z,\chi_{st}) dZ d\chi_{st}$, where $P(Z,\chi_{st})$ is a joint probability-density function (PDF) which needs modeling, and which represents subgrid mixing and straining processes that cannot be captured in RANS or LES. Models of $P(Z,\chi_{st})$ are normally made to depend on $\widetilde{Z}$, $\widetilde{Z''^2}$ and χ_{st} (Peters 2000), and solutions of the type $\widetilde{\Psi}_{i,f}(\widetilde{Z},\widetilde{Z''^2},\chi_{st})$ can be pre-computed and retrieved during the simulations to calculate the local composition, temperature, density and thermodynamic coefficients depending on the local values of $\widetilde{Z}$, $\widetilde{Z''^2}$ and χ_{st}. However, because of the multivalued character of the bifurcation curve in Figure 1(b), steady non-premixed flamelets are only capable of capturing the vigorously-burning branch up to the extinction point, following the frozen branch thereon, as depicted in Figure 1(b). Regions of re-ignition, premixing or preheating cannot therefore be described by steady non-premixed flamelets.

To compensate for the inaccessibility of the steady non-premixed flamelets to the lower branch and the ignition point, which may be of some interest to capture in partially-premixed zones such as near-injector regions in high-speed combustors of the type originally analyzed by Pierce & Moin (2004) (i.e., with inlet speeds much larger than the laminar premixed-flame velocity), a remapping of the flamelet solution was proposed in earlier work in terms of an additional progress variable C, which represents the degree of completion of the combustion process. This treatment was termed the flamelet progress-variable approach (FPVA) (Pierce & Moin 2004). When the mass fractions and temperature are mapped onto Z and C, the multivalued character of the $Z-\chi_{st}$ parametrization disappears. Therefore, access to the middle and lower branch up to the ignition point is granted, as depicted in Figure 1(b) by the solid-line trajectory. However, it should be noted that the middle branch is believed to be unstable (Williams 1985), and therefore the physical relevance of capturing the middle branch could be questioned. The average or filtered values of the flamelet variables $\Psi_{i,f}$ then become $\widetilde{\Psi}_{i,f} = \int \Psi_{i,f} P(Z,C) dZ dC$. Since C is not a passive scalar, an additional conservation equation for C is required, in which the source term $\dot{w}_C$ requires closure upon averaging or filtering. The averaged/filtered progress-source term becomes $\widetilde{\dot{w}}_C = \int \dot{w}_C P(Z,C) dZ dC$ and solutions of the type $\widetilde{Y}_k(\widetilde{Z},\widetilde{Z''^2},\widetilde{C})$, $\widetilde{T}(\widetilde{Z},\widetilde{Z''^2},\widetilde{C})$ and $\widetilde{\dot{w}}_C(\widetilde{Z},\widetilde{Z''^2},\widetilde{C})$ can be pre-computed and read during numerical simulations. Nonetheless, it should be emphasized that the ignition point I in Figure 1(b) is not indicative of autoignition in the evolution-type of flows normally found in practical applications, in which two streams of fuel and oxidizer ignite only when they mix together at sufficiently high temperatures and after decomposition of heavy fuel molecules into a large amount of radicals, and in which the prediction of autoignition requires careful consideration of the reactant time-histories as opposed to the quasi-static treatment that leads to Figure 1(b). Despite these limitations, the steady FPVA model allows for a simple representation of quasi-static ignition in terms of the instantaneous-filtered or averaged local strain value.

Earlier studies have analyzed the effects of chemical uncertainties in simple combustion problems, such as single-step ignition and planar flame propagation (Najm *et al.* 2009). A recent study (Mueller *et al.* 2012) tackled a more complex problem by investigating

the effects of chemical-rate uncertainties in LES of an unconfined and piloted low-Mach methane-air jet diffusion flame, which represents a configuration suitable to be modeled by steady non-premixed flamelets. The methodology proposed in that study is extended below to high-speed partially-premixed turbulent reacting flows. This analysis makes use of the concept of "gates" in uncertainty quantification (Iaccarino *et al.* 2012), by which the stochastic space is reduced in the direction of the uncertainty arrow by taking advantage of the disparity of scales, as depicted in Figure 1(a).

3. Transport equations in the RANS-FVPA framework

In the RANS context, the aerothermochemical variables are decomposed as $f = \widetilde{f} + f''$, where $\widetilde{f}$ is a Favre average and f'' is the perturbation. When the time-averaging operator is applied to the Navier-Stokes equations and the transported variables are decomposed into Favre-mean and Favre-perturbations, and under a number of assumptions detailed below, the conservation equations become

$$\frac{\partial \overline{\rho}}{\partial t} + \boldsymbol{\nabla}\cdot(\overline{\rho}\widetilde{\boldsymbol{v}}) = 0, \tag{3.1}$$

$$\frac{\partial \overline{\rho}\widetilde{\boldsymbol{v}}}{\partial t} + \boldsymbol{\nabla}\cdot(\overline{\rho}\widetilde{\boldsymbol{v}}\widetilde{\boldsymbol{v}}) = -\boldsymbol{\nabla}\overline{p} + \boldsymbol{\nabla}\cdot\overline{\boldsymbol{\tau}} - \boldsymbol{\nabla}\cdot(\overline{\rho}\widetilde{\boldsymbol{v}''\boldsymbol{v}''}), \tag{3.2}$$

$$\frac{\partial \overline{\rho}\widetilde{Z}}{\partial t} + \boldsymbol{\nabla}\cdot(\overline{\rho}\widetilde{\boldsymbol{v}}\widetilde{Z}) = \boldsymbol{\nabla}\cdot(\overline{\rho D}\boldsymbol{\nabla}\widetilde{Z}) - \boldsymbol{\nabla}\cdot(\overline{\rho}\widetilde{\boldsymbol{v}''Z''}), \tag{3.3}$$

$$\frac{\partial \overline{\rho}\widetilde{C}}{\partial t} + \boldsymbol{\nabla}\cdot(\overline{\rho}\widetilde{\boldsymbol{v}}\widetilde{C}) = \boldsymbol{\nabla}\cdot(\overline{\rho D}\boldsymbol{\nabla}\widetilde{C}) - \boldsymbol{\nabla}\cdot(\overline{\rho}\widetilde{\boldsymbol{v}''C''}) + \overline{\rho}\widetilde{\dot{w}}_C, \tag{3.4}$$

$$\begin{aligned}\frac{\partial \overline{\rho}\widetilde{Z''^2}}{\partial t} + \boldsymbol{\nabla}\cdot(\overline{\rho}\widetilde{\boldsymbol{v}}\widetilde{Z''^2}) = {} & -2\overline{\rho}\widetilde{\boldsymbol{v}''Z''}\boldsymbol{\nabla}\widetilde{Z} - \boldsymbol{\nabla}\cdot(\overline{\rho}\widetilde{\boldsymbol{v}''Z''^2}) + 2\overline{Z''\boldsymbol{\nabla}\cdot(\rho D\boldsymbol{\nabla}\widetilde{Z})} \\ & + \boldsymbol{\nabla}\cdot(\overline{\rho D}\boldsymbol{\nabla}\widetilde{Z''^2}) - 2\overline{\rho D(\boldsymbol{\nabla}Z'')^2},\end{aligned} \tag{3.5}$$

$$\frac{\partial \overline{\rho}\widetilde{E}}{\partial t} + \boldsymbol{\nabla}\cdot(\overline{\rho}\widetilde{\boldsymbol{v}}\widetilde{E}) = -\boldsymbol{\nabla}\cdot(\overline{p}\overline{v}) + \boldsymbol{\nabla}\cdot(\overline{\tau}\overline{v}) - \boldsymbol{\nabla}\cdot(\overline{\rho}\widetilde{\boldsymbol{v}''E''}) - \boldsymbol{\nabla}\cdot\overline{\boldsymbol{q}}, \tag{3.6}$$

which are listed here for reference. In this formulation, p is the pressure, $\boldsymbol{\tau}$ is the viscous stress tensor and $\boldsymbol{q}$ is the heat flux. Similarly, C is a progress variable that is typically taken to be the main combustion product. Additionally, $\widetilde{E} = \widetilde{e} + \widetilde{\boldsymbol{v}}\cdot\widetilde{\boldsymbol{v}}^{\mathrm{T}}/2 + k$ is the Favre mean of the total energy, with k being the turbulent kinetic, $\widetilde{e} = \widetilde{h} + \overline{p}/\overline{\rho}$ the internal energy, and

$$\widetilde{h} = \sum_{k=1}^{N}\widetilde{Y}_k h_k^0 + \sum_{i=1}^{N}\int_{T^0}^{\widetilde{T}}\widetilde{Y}_k c_{p,k}dT \tag{3.7}$$

the enthalpy, where $c_{p,k}$ is the specific heat at constant pressure of species k and N is the number of species. Additionally, the equation of state

$$\overline{p} = \overline{\rho}\widetilde{R}\widetilde{T}, \quad \text{with} \quad \widetilde{R} = R^0\sum_{k=1}^{N}\widetilde{Y}_k/W_k, \tag{3.8}$$

is used to calculate the mean pressure $\overline{p}$, with R^0 the universal gas constant and W_k the molecular weight of species k. In high-speed reacting flows, the temperature $\widetilde{T}$ in (3.7) and (3.8) should not be confused with the flamelet temperature, as stressed below.

Equations (3.2)-(3.6) require closure. When traditional Boussinesq-type closure models are used for the turbulent fluxes, eqs. (1)-(6) in Pecnik *et al.* (2012) are recovered.

Some approximations were undertaken when writing eqs. (3.3)-(3.5), (3.7) and (3.8), which are worth highlighting in the present context of uncertainty quantification, and because it may be erroneously believed that these equations are exact even before undertaking any endeavors for modeling the unclosed terms. In particular, eq. (3.3) was derived under the assumption that all the molecular diffusivities in the mixture are equal, $D_k = D$, in which case (3.3) can be obtained by linearly combining the species conservation equations. If the molecular diffusivities are not equal, a transport equation for $\widetilde{Z}$ similar to (3.3) can be written (Peters 2000), but it becomes physically unclear what molecular diffusivity must be used in (3.3) -which in turn needs to be a calibrated diffusivity- or whether the stoichiometric mixture fraction is in any physical way related to the flame location in the fast-chemistry sense as it is when all the mass diffusivities are equal. Similarly, the Favre-averaging operator was made to commute with the definite integral sign in the second term of (3.7), and the same operator was also split in the product of the mass fractions and the temperature in the equation of state (3.8); these approximations are suspect to degrade the solution if the correlations $\widetilde{Y_k''T''}$ are not small, which is typically the case in combustion (Peters 2000).

4. A stochastic FPVA formulation under chemical-kinetic uncertainties

Additional closures are required for the thermodynamic coefficients, Favre-averaged mass fraction and progress-variable source term in (3.1)-(3.8), which are obtained via flamelet modeling by integrating the steady problem

$$\frac{\chi}{2}\frac{\partial^2 Y_{k,f}}{\partial Z^2} = -\dot{w}_{k,f}, \tag{4.1}$$

$$\frac{\chi}{2}\frac{\partial^2 T_f}{\partial Z^2} = \sum_{k=1}^{N}\frac{h_k^0 \dot{w}_{k,f}}{c_{p,f}}, \tag{4.2}$$

which is given here in a simpler form for space constraints. The two flamelet conservation equations typically integrated are listed in Pitsch & Peters (1998), which include the effects of multi-species diffusion and different $c_{p,k}$ among chemical species. Equations (4.1) and (4.2) are subject to the boundary conditions

$$Y_{k,f} = Y_{i,\mathrm{F}} \quad \text{and} \quad T_f = T_{\mathrm{F,F}}, \tag{4.3}$$

in the fuel stream $Z = 1$, and

$$Y_{k,f} = Y_{i,\mathrm{A}} \quad \text{and} \quad T_f = T_{\mathrm{A}}, \tag{4.4}$$

in the air stream $Z = 0$. The subindex $_f$ has been used here to denote the variables obtained from the solution to the flamelet problem (4.1)-(4.4). In this formulation, $\dot{w}_{k,f}$ is the chemical production of species k. In particular, for $k = C$, the progress-variable source term $\dot{w}_{C,f}$ is obtained. Similarly, $\chi = 2D|\nabla Z|^2$ is the scalar dissipation rate, a closure model for which can be obtained, for instance, by deriving and squaring eq. (5) in Liñán (1974) for the thermodiffusive case. The stoichiometric scalar dissipation rate χ_{st} is usually obtained from the outer field by using the approximate eq. (3.157) in Peters (2000). In an asymptotic sense, the inner-problem formulation (4.1)-(4.4) is valid up to scales of order ℓ_m, as depicted in Figure 1(a).

In the deterministic FPVA model, key Favre-averaged variables such as $\widetilde{T}_f$, $\widetilde{\dot{w}}_{C,f}$, $\widetilde{e}_f$, $\widetilde{\gamma}_f$, $d\widetilde{\gamma}/d\widetilde{T}$, $\widetilde{R}_f$, $\widetilde{\mu}_f$, and $\widetilde{\lambda/c_p}|_f$ are pre-computed in chemical tables as a function of $\widetilde{Z}$, $\widetilde{C}$ and $\widetilde{Z''^2}$ by convoluting the solution of (4.1)-(4.4) with PDF models, as outlined in Section 2, and then they are injected to the outer-problem formulation (3.1)-(3.8). Here μ is the dynamic viscosity and λ the thermal conductivity.

Equations (4.1)-(4.4) are subject to the equation of state (3.8) without the averaging operator. In the low-Mach number limit used to describe flamelets by (4.2), the background pressure remains uniform in scales of order ℓ_m. The flamelets can be computed at constant pressure p, which in turn requires a scaling correction in the progress-variable source term in (3.4) if read directly from the table (Pecnik *et al.* 2012), or they can be computed at different pressures, thereby considering the pressure p as a tabulation input. The analysis below considers the second approach, which is the most general one, and it automatically simplifies to the single-pressure case when only one value of the pressure is used to precompute flamelets.

4.1. *An uncertainty-aware chemical table*

In this investigation, the FPVA model is extended to tackle uncertainties in the chemical reaction rates. Consider, without any loss of generality, a chemical mechanism in which the vector of chemical rate constants $\boldsymbol{\mathcal{K}} = [k_{f,1}, \ldots, k_{f,M}]$ in a kinetic mechanism of M elementary steps is given by the general expression (3.2) in Urzay *et al.* (2012), namely,

$$\ln \boldsymbol{\mathcal{K}} = \boldsymbol{\mathcal{G}}[\boldsymbol{\mathcal{S}}(\boldsymbol{\xi_{in}}), p, T] \quad \text{and} \quad \boldsymbol{\mathcal{S}} = \boldsymbol{\mathcal{F}}(\boldsymbol{\xi_{in}}), \tag{4.5}$$

where $\boldsymbol{\mathcal{G}}$ and $\boldsymbol{\mathcal{F}}$ are operators defined in Section 3 of Urzay *et al.* (2012), and $\boldsymbol{\xi}_{in}$ is a $\mathbb{R}^{L\times 1}$ vector of independent random variables used to describe the input random space, with $L \geq M$ in general. The operator $\boldsymbol{\mathcal{F}}$ can be obtained analytically or evaluated numerically by using any of the methods $\mathcal{M}_1 - \mathcal{M}_4$ described in Urzay *et al.* (2012).

In this stochastic FPVA model and for a single realization of $\boldsymbol{\mathcal{K}}$, the value of a generic variable $\Psi_{i,f}$ read from the flamelet table can be written as

$$\widetilde{\Psi}_{i,f}(\widetilde{Z}, \widetilde{Z''^2}, \widetilde{C}, \overline{p}, \boldsymbol{\mathcal{K}}) = \int \Psi_i(C, Z, \boldsymbol{\mathcal{K}}, p)\widetilde{P}(Z, C, p)dZdC_f dp, \tag{4.6}$$

for averaged and Favre-averaged variables, respectively. In this formulation, $\widetilde{P}(Z, C, p) = \widetilde{P}(\{Z, C\}|p)P(p)$ is the density-weighted joint PDF which models the turbulence effects on the flamelets. In particular, one could assume that Z is independent of p to a good extent, and therefore write $\widetilde{P}(Z, C, p) = \widetilde{P}(Z)P(C|\{Z, p\})P(p)$. In particular, $\widetilde{P}(Z)$ is a micro-mixing PDF usually modeled as a beta function parametrized by $\widetilde{Z}$ and $\widetilde{Z''^2}$. The PDF of the pressure $P(p)$ is assumed to be a delta function $\delta(p - \overline{p})$ centered at the average pressure $\overline{p}$. Similarly, $\widetilde{P(C|\{Z, p\})}$ is a conditional PDF modeled as a delta function $\delta(C - \widetilde{C|\{Z, p\}})$, where $C|\{Z, p\}$ is the flamelet solution $C(Z, \chi'_{st}, \overline{p})$, where χ'_{st} is a scalar dissipation rate chosen to enforce the constraint

$$\widetilde{C} = \widetilde{C}_f = \int C(Z, \chi'_{st}, \overline{p})\tilde{P}(Z)dZ, \tag{4.7}$$

in such a way that the flamelet solution and the solution given by the progress-variable transport equation (3.4) are consistent. By enforcing the consistency condition (4.7), χ'_{st} may not be necessarily related to the scalar dissipation rate that would be obtained from the solution of the transport equations (3.1)-(3.6) (Pierce & Moin 2004).

It is worth emphasizing that if C is taken to be the water-vapor mass fraction in

hydrogen combustion, in the autoignition region of Figure 1(a), the water-vapor mass fraction obtained from an unsteady version of the flamelet problem (4.1)-(4.3) would be smaller than the progress variable obtained by the steady flamelet solution, all numerical errors aside, the reason being that the flamelet solution does not account for the chemical inertia involved in the decomposition of large fuel molecules and subsequent radical build up that occurs upon autoignition. In other words, during autoignition of hydrogen flames, even though the autoignition process occurs across spatial scales of the same order as the microscale ℓ_m, there is no time-scale separation that permits matching the solution of the unsteady outer problem (3.1)-(3.8) with the solution of the steady inner problem (4.1)-(4.4), since autoignition occurs in time scales of the same order as the integral time scale ℓ/U. As a consequence, if the chemical table was fed with the exact progress variable, the scalar dissipation rate viewed by the chemical table would be in fact larger than the scalar dissipation rate observed from the resolution of the conservation equations.

In this FPVA model applied to high-speed combustion, the averaged variables (4.6) are sole functions of the mixture fraction $\widetilde{Z}$, mixture-fraction variance $\widetilde{Z''^2}$, average pressure $\overline{p}$ and progress variable $\widetilde{C}$, the three of which represent input variables for the chemical table. However, note that (4.6) requires one chemical table per realization in the random rate constants $\boldsymbol{\mathcal{K}}$. In general, the limiting factor of uncertainty quantification of turbulent flows is the computational cost of the individual resolutions of the aerothermochemical transport equations at each realization in the reaction-rate space. From the practical standpoint, the brute-force approach may require a large computational cost, especially in the case of LES and for heavy-hydrocarbon fuels, for which the chemical mechanisms have many elementary steps (approximately as many as $M = 784$ steps for JP-7). However, for chemical-kinetic uncertainty quantification with relatively simpler fuels, such as hydrogen, the number of random outputs from the chemical table (which typically amount to 8 outputs as shown below) may become similar or larger than the number of random input variables L needed to describe uncertainties in the mechanism if reduced chemistry is employed (a minimum of $L = 9$ random inputs are required for the 3-step reduced H_2/O_2 mechanism of Boivin *et al.* (2011)). The methodology presented in this study provides an attractive lower-cost alternative to the brute-force approach in systems in which $L > 8$ by making use of the concept of "gate" (Iaccarino *et al.* 2012), in that a dimension reduction in the random-variable space is made through the flamelet approximation by transferring all the uncertainties from the L-dimensional input random space of random chemical rates $\boldsymbol{\mathcal{K}}$ to a downsized $D-$dimensional stochastic space of chemical-table outputs, with $D \ll M \leq L$. Additionally, the indirect uncertainties caused by the stochastic output variables on the transported aerothermochemical variables do not revert to the chemical table. This method is described below.

A single chemical table can be pre-computed which contains statistical moments of the output variables $\widetilde{\Psi}_{i,f}$. In particular, the mean and variance of the flamelet variable over the stochastic space $\boldsymbol{\mathcal{K}}$ are given by

$$\mathrm{E}[\widetilde{\Psi}_{i,f}] = \int \Psi_{i,f} \tilde{P}(Z, C, p, \boldsymbol{\mathcal{K}}) dZ dC dp d\boldsymbol{\mathcal{K}}, \tag{4.8}$$

and

$$\mathrm{cov}[\widetilde{\Psi}_{i,f}, \widetilde{\Psi}_{j,f}] = \int (\Psi_{i,f} - \mathrm{E}[\widetilde{\Psi}_{i,f}])(\Psi_{j,f} - \mathrm{E}[\widetilde{\Psi}_{i,f}]) \widetilde{P}(Z, C, p, \boldsymbol{\mathcal{K}}) dZ dC dp d\boldsymbol{\mathcal{K}}, \tag{4.9}$$

where

$$\widetilde{P}(Z, C, p, \boldsymbol{\mathcal{K}}) = \widetilde{P}(\{Z, C, p\}|\boldsymbol{\mathcal{K}}) P(\boldsymbol{\mathcal{K}}) \tag{4.10}$$

is a joint PDF. In this formulation, the symbols E[·] and cov[·] represent mean and covariance in the $\boldsymbol{\mathcal{K}}$-space conditioned on the pressure, respectively. If the flamelets are computed at a single pressure, the pressure conditioning disappears and E[·] and cov[·] are just the mean and covariance in the reaction-rate space.

Further assumptions are needed to model the conditional PDF $P(\{Z, C, p\}|\boldsymbol{\mathcal{K}})$ in (4.10). First, the mixture fraction Z is assumed to be independent of the random reaction rates and of the pressure, since in the mixture-fraction formulation (4.1)-(4.4) of the flamelet equations, Z becomes an independent coordinate. Additionally, in the low-Mach flamelet formulation (4.1)-(4.4), the pressure p represents an input parameter, and therefore it can be taken to be independent of the rates. On the other hand, the progress variable C is a solution of the flamelet equations. If, as per usual in practice, C is taken to be the product mass fraction to avoid multi-valued mapping, it is evident that C and $\boldsymbol{\mathcal{K}}$ must be dependent, since $C = 0$ for $\boldsymbol{\mathcal{K}} = 0$. Under these assumptions $P(\{Z, C, p\}|\boldsymbol{\mathcal{K}})$ can be written as

$$\widetilde{P}(\{Z, C, p\}|\boldsymbol{\mathcal{K}}) = \widetilde{P}(Z)P(p)(P(C|\{Z, p, \boldsymbol{\mathcal{K}}\}), \tag{4.11}$$

where $P(Z)$ is modeled by the beta PDF, $P(p) = \delta(p - \overline{p})$, and $P(C|\{Z, \boldsymbol{\mathcal{K}}\})$ is modeled as

$$P(C|\{Z, p, \boldsymbol{\mathcal{K}}\}) = \delta(C - C|\widetilde{\{Z, p,} \boldsymbol{\mathcal{K}}\}) \tag{4.12}$$

centered at $C|\widetilde{\{Z, p,} \boldsymbol{\mathcal{K}}\} = C(Z, \chi_{st}, \overline{p}, \boldsymbol{\mathcal{K}})$. Upon substituting these expressions in (4.6)-(4.8), the equations

$$\mathrm{E}[\widetilde{\Psi}_{i,f}](\widetilde{Z}, \widetilde{Z''^2}, \mathrm{E}[\widetilde{C}], \overline{p}) = \int \Psi_{i,f}(Z, \mathrm{E}[\widetilde{C}], p)\widetilde{P}(Z)dZ, \tag{4.13}$$

$$\mathrm{cov}[\widetilde{\Psi}_{i,f}, \widetilde{\Psi}_{j,f}](\widetilde{Z}, \widetilde{Z''^2}, \mathrm{E}[\widetilde{C}], \overline{p}) = \mathrm{E}[\widetilde{\Psi}_{i,f}\widetilde{\Psi}_{j,f}] - \mathrm{E}[\widetilde{\Psi}_{i,f}]\mathrm{E}[\widetilde{\Psi}_{j,f}] \tag{4.14}$$

are obtained, where

$$\mathrm{E}[\widetilde{C}](\widetilde{Z}, \widetilde{Z''^2}, \chi_{st}, \overline{p}) = \int C(Z, \chi_{st}, \overline{p}, \boldsymbol{\mathcal{K}})\widetilde{P}(Z)P(\boldsymbol{\mathcal{K}})dZd\boldsymbol{\mathcal{K}} \tag{4.15}$$

is the conditional mean of the Favre-averaged progress variable over the stochastic reaction-rate space conditioned on the average external pressure $\overline{p}$.

For numerical purposes, it is more expedient to express eqs. (4.13)- (4.15) in a discretized form using a quadrature rule for the integration in Z, which gives

$$\mathrm{E}[\widetilde{\Psi}_{i,f}](\widetilde{Z}, \widetilde{Z''^2}, \mathrm{E}[\widetilde{C}], \overline{p}) = \sum_{k=1}^{Q} \omega_k \mathrm{E}[\Psi_{i,f}(Z_k, \mathrm{E}[\widetilde{C}], \boldsymbol{\mathcal{K}})], \tag{4.16}$$

$$\begin{aligned}
&\mathrm{cov}[\widetilde{\Psi}_{i,f}, \widetilde{\Psi}_{j,f}](\widetilde{Z}, \widetilde{Z''^2}, \mathrm{E}[\widetilde{C}], \overline{p}) \\
&= \sum_{k=1}^{Q} \omega_k^2 \mathrm{cov}[\Psi_{i,f}(Z_k, \mathrm{E}[\widetilde{C}], \overline{p}, \boldsymbol{\mathcal{K}}), \Psi_{j,f}(Z_k, \mathrm{E}[\widetilde{C}], \overline{p}, \boldsymbol{\mathcal{K}})] \\
&+ \sum_{k=1}^{Q} \sum_{m=k+1}^{Q} \omega_k \omega_\ell \Big\{ \mathrm{cov}[\Psi_{i,f}(Z_k, \mathrm{E}[\widetilde{C}], \overline{p}, \boldsymbol{\mathcal{K}}), \Psi_{j,f}(Z_m, \mathrm{E}[\widetilde{C}], \overline{p}, \boldsymbol{\mathcal{K}})] \\
&\quad + \mathrm{cov}[\Psi_{i,f}(Z_m, \mathrm{E}[\widetilde{C}], \overline{p}, \boldsymbol{\mathcal{K}}), \Psi_{j,f}(Z_k, \mathrm{E}[\widetilde{C}], \overline{p}, \boldsymbol{\mathcal{K}})] \Big\},
\end{aligned} \tag{4.17}$$

and

$$\mathrm{E}[\widetilde{C}](\widetilde{Z},\widetilde{Z''^2},\chi_{st},\overline{p})=\sum_{k=1}^{Q}\omega_k\mathrm{E}[C(Z_k,\chi_{st},\overline{p},\boldsymbol{\mathcal{K}})], \tag{4.18}$$

where Q is the number of quadrature points and ω_k are integration weights (which depend on the local value of $\widetilde{Z}$ and $\widetilde{Z''^2}$).

In this formulation, the stochastic $\boldsymbol{\mathcal{K}}$-space statistics $\mathrm{E}[\widetilde{\Psi}_{i,f}]$ and $\mathrm{cov}[\widetilde{\Psi}_{i,f},\widetilde{\Psi}_{j,f}]$ are parametrized in terms of $\widetilde{Z}$, $\widetilde{Z''^2}$ and $\mathrm{E}[\widetilde{C}]$ (and not $\widetilde{C}$). The fact that C is used here as a mapping variable instead of χ_{st} poses a fundamental challenge in the present investigation that did not exist in earlier work by Mueller *et al.* (2012) on steady non-premixed flamelets. In steady non-premixed flamelets, the scalar dissipation rate at stoichiometry χ_{st} is an independent parameter upon which the manifold of flamelet solutions is discretized. Therefore the joint PDF $\widetilde{P}(Z,\chi_{st},\boldsymbol{\mathcal{K}})$ is simply equal to $\widetilde{P}(Z)P(\chi_{st})P(\boldsymbol{\mathcal{K}})$. As a result, the mean of a flamelet variable over the stochastic $\boldsymbol{\mathcal{K}}$ space becomes a sole function of $\widetilde{Z}$, $\widetilde{Z''^2}$ and $\widetilde{\chi}_{st}$, the three of which are discretized independently as inputs for the chemical table and do not contain any direct source of randomness from $\boldsymbol{\mathcal{K}}$ (Mueller *et al.* 2012). However, in the FPVA approach, the progress variable C is a solution of the flamelet equations and C is directly influenced by randomness from the $\boldsymbol{\mathcal{K}}$ variations. In fact, different realizations in the $\boldsymbol{\mathcal{K}}$ space yield different surfaces $\widetilde{C}=\widetilde{C}(\widetilde{Z},\widetilde{Z''^2},\chi_{st},\overline{p})$. Therefore, the mean surface $\mathrm{E}[\widetilde{C}]=\mathrm{E}[\widetilde{C}](\widetilde{Z},\widetilde{Z''^2},\chi_{st},\overline{p})$ appears naturally as a tabulation input, which is calculated as the mean of $\widetilde{C}$ over the $\boldsymbol{\mathcal{K}}-$space for a given average external pressure $\overline{p}$.

This treatment may lead to an inconsistency between the transported progress variable $\widetilde{C}$ obtained by solving the transport equation (3.4), and the mean progress variable $\mathrm{E}[\widetilde{C}]$, which is obtained from the $\boldsymbol{\mathcal{K}}-$averaged chemical table. If the table based on mean variables over the $\boldsymbol{\mathcal{K}}-$space is used in a single calculation, in principle there is no warranty that the $\widetilde{C}$-field obtained from the integration of the progress-variable transport eq. (3.4) matches the mean progress variable $\mathrm{E}[\widetilde{C}]$ from the flamelet table. This discrepancy cannot be solved by averaging in the $\boldsymbol{\mathcal{K}}$-space the Favre-averaged conservation eqs. (3.1)-(3.8), since such approach would produce crossed terms of unknown nature. Notwithstanding these limitations, an analogous consistency condition to (4.7) may be enforced by choosing an appropriate scalar dissipation χ''_{st} such that $\widetilde{C}=\mathrm{E}[\widetilde{C}]$, or equivalently, by using (4.15) to give

$$\widetilde{C}=\int C(Z,\chi''_{st},\overline{p},\boldsymbol{\mathcal{K}})\widetilde{P}(Z)P(\boldsymbol{\mathcal{K}})dZd\boldsymbol{\mathcal{K}}. \tag{4.19}$$

However, the physical implications of the choice of χ''_{st} in (4.19) are more obscure in comparison with the physical implications of the choice of χ'_{st} in (4.7). Equation (4.19) should be taken as the leading-order approximation for small amplitudes of the variations in the $\boldsymbol{\mathcal{K}}$ space, for which the quantity $|\chi''_{st}-\chi'_{st}|/\chi'_{st}$ is expected to be small, thereby making the constraint (4.19) at least as physically reasonable as it was in the deterministic case.

4.2. *Stochastic computation of the temperature in high-speed turbulent-reacting flows*

At low Mach numbers, the background pressure remains constant and the density becomes a sole function of the mixture composition and the temperature. In the steady non-premixed flamelet approach, the energy and progress-variable eqs. (3.4) and (3.6) are not integrated in the outer problem. Alternatively, the density $\overline{\rho}(\widetilde{Z},\widetilde{Z''^2},\chi_{st})$ and the

molecular coefficients are retrieved from the chemical table (Mueller *et al.* 2012). Similarly, the temperature $\widetilde{T}$ can either be obtained from the table or from the equation of state (3.8) based on the flamelet density and flamelet mass fractions up to errors related to the splitting of the Favre operator in (3.8).

At moderate to high Mach numbers, an additional contribution to the discrepancy between $\widetilde{T}$ and $\widetilde{T}_f$ comes from the fact that the kinetic energy becomes of the same order as the thermal energy. The total-energy equation (3.6) is typically integrated for facilitating the treatment of shock waves in terms of conserved fluxes. However, at such high speeds the excess of kinetic energy in the flow renders the outer enthalpy $\widetilde{h}$ generally different from the flamelet enthalpy $\widetilde{h}_f$ in amounts of the same order as the large-scale kinetic energy, especially if the flamelets are computed at constant pressure, which leads to dimensionless differences $|\widetilde{T}-\widetilde{T}_f|/\widetilde{T}_f$ of the same order as the Mach number squared. In fact, the validity of the flamelet approach at high convective Mach numbers -in which compressibility effects start becoming important within the mixing microscales of Figure 1(b)- is questionable, since the flamelet formulation integrates a low-Mach number set of conservation equations in the microscale.

To partially compensate for the detrimental effects of compressibility in the approximation $\widetilde{T} \sim \widetilde{T}_f$, the temperature is computed here by using the method described in Pecnik *et al.* (2012). In that method, the enthalpy equation (3.7) is rewritten as $\widetilde{h}-\widetilde{h}_f = \int_{\widetilde{T}_f}^{\widetilde{T}} \widetilde{c}_p dT$ and integrated for a slowly varying average adiabatic coefficient $\widetilde{\gamma} \sim \widetilde{\gamma}_f + a_{\widetilde{\gamma}}(\widetilde{T}-\widetilde{T}_f)$ and for the case in which $\widetilde{R}$ remains constant with temperature, where $\widetilde{h}_f = \sum_{k=1}^{N} Y_k h_k^0 + \int_{T^0}^{\widetilde{T}_f} \widetilde{c}_p dT$ is the flamelet enthalpy, $\widetilde{c}_p = \sum_{k=1}^{N} \widetilde{Y}_k c_{p,k} = \widetilde{\gamma}\widetilde{R}/(\widetilde{\gamma}-1)$ is the average specific heat at constant pressure, $\widetilde{\gamma} = \widetilde{c}_p/\widetilde{c}_v$ is the average adiabatic coefficient, and $a_{\widetilde{\gamma}} = d\widetilde{\gamma}/d\widetilde{T}$. Using these approximations, the Favre-average temperature becomes

$$\widetilde{T} = \widetilde{T}_f + \frac{\widetilde{\gamma}_f - 1}{a_{\widetilde{\gamma}}} \left\{ \exp\left[\frac{a_{\widetilde{\gamma}}(\widetilde{e}-\widetilde{e}_f)}{\widetilde{R}_f} \right] - 1 \right\} \tag{4.20}$$

which, as suggested by (Pecnik *et al.* 2012), seems to deviate less than 5 K from the solution obtained by solving (3.7) for small differences $|\widetilde{T}-\widetilde{T}_f|$. As outlined in the following section, all the flamelet variables on the right hand side of (4.20) are in principle stochastic because of the randomness in the $\boldsymbol{\mathcal{K}}$ space, in a manner described by eq. (4.6). Similarly, the Favre-averaged internal energy $\widetilde{e}$ is also stochastic since it is one of the solution variables to the problem (3.1)-(3.8). The utilization of eq. (4.20) is therefore attractive in that the mass fractions $\widetilde{Y}_k$ do not need to be retained as outputs of the chemical table and therefore they do not need to be sampled.

5. Propagation of chemical-kinetic uncertainties

Figure 2 is a self-explanatory flowchart that describes the algorithm of the method described in the previous section. As described above, the method reduces an $L-$dimensional stochastic space of input random variables $\boldsymbol{\xi_{in}}$, which are needed to describe the uncertainties in the rate-constants of a chemical mechanism of M elementary steps, to a D-dimensional stochastic space $\boldsymbol{\xi_{out}}$ needed to describe the output random variables from the chemical table. The method uses two gates: the chemical-kinetics gate and the flamelet gate. The chemical kinetics gate is a one-way gate above which the chemical-kinetics uncertainty is characterized as in Urzay *et al.* (2012) independently of the rest of

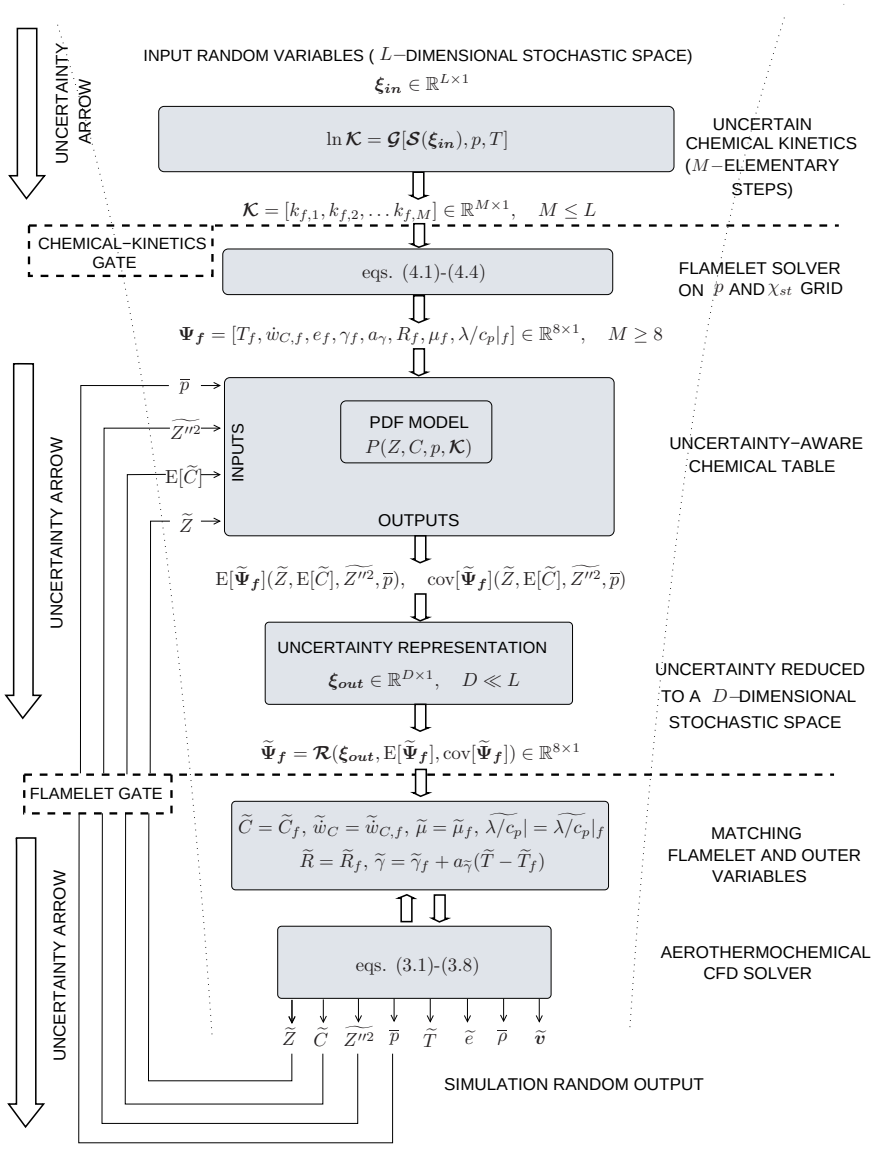

FIGURE 2. Flowchart of the flamelet progress-variable approach for high-speed turbulent combustion under chemical-kinetic uncertainties.

the problem. At this first level, reduction of the input-uncertainty space can be performed by expert opinion or by sensitivity analyses. At the flamelet gate, the uncertainties in the high-dimensional random input space are reduced to uncertainties in the output variables from the table. Obviously, this strategy only makes sense in terms of computational-cost savings when large chemical mechanisms in which $L \gg D$ are used. The reduction of uncertainties at the flamelet gate is again independent of the outer problem and can be performed by analyzing the sample space of the stochastic flamelets, from which a model for the operator $\boldsymbol{\mathcal{R}}$ can be derived. In a hierarchical construction of uncertainty models

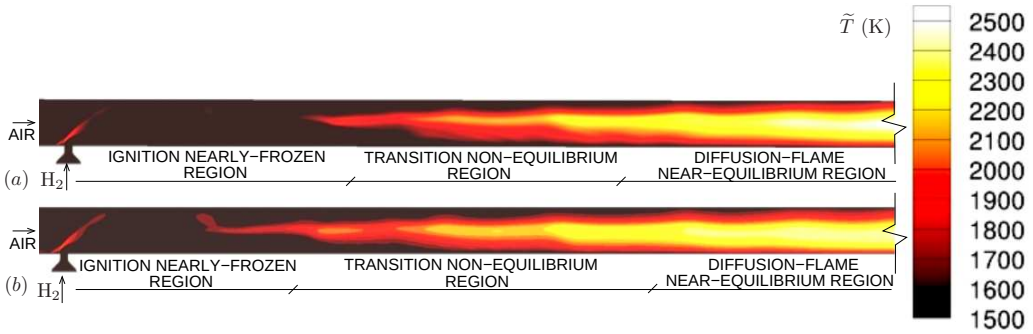

FIGURE 3. Deterministic RANS numerical simulations of the HyShot-II SCRAMJET engine for (a) non-diluted H_2-stream, and (b) 70% diluted H_2-stream with N_2. The figures show less than half of the total length of the combustor.

at the flamelet gate, simple models for the operator $\boldsymbol{\mathcal{R}}$ of the type

$$\widetilde{\Psi}_{f,i} = \mathcal{R}_i(\boldsymbol{\xi_{out}}, \mathrm{E}[\widetilde{\boldsymbol{\Psi}}_{\boldsymbol{f}}], \mathrm{cov}[\widetilde{\boldsymbol{\Psi}}_{\boldsymbol{f}}]) = \mathrm{E}[\widetilde{\Psi}_{f,i}] + \sqrt{\mathrm{var}[\widetilde{\Psi}_{f,i}]}\xi_i, \tag{5.1}$$

can be proposed for the relevant flamelet variables, where the conditional mean and variances of $\Psi_{f,i}$ are calculated in the $\boldsymbol{\mathcal{K}}-$space conditioned on the tabulated pressure $\overline{p}$. In the first approximation the mean response of the overall turbulent-combustion computation may be approximated by integrating (3.1)-(4.4) based on mean table quantities if statistical non-linearities are neglected in the commutation of mean operators. However, the model (5.1) neglects correlations between flamelet variables $\widetilde{\Psi}_{f,i}$, which contradicts physical intuition. Further research is underway to obtain physics-constrained models for the operator $\boldsymbol{\mathcal{R}}$.

6. A note on the potential effects of chemical-kinetic uncertainties in the HyShot-II SCRAMJET engine

A case study for the effects of chemical-kinetic uncertainties in supersonic combustion that has provoked some interest recently is the HyShot-II supersonic-combustion ramjet (SCRAMJET). Figure 3 shows temperature contours from deterministic RANS simulations of HyShot-II. The details of the numerical solver are given elsewhere (Pecnik *et al.* 2012).

In the combustor of HyShot-II, a sonic jet of hydrogen (H_2) at $T_{H_2,F} = 213$ K is injected in a crossflow with respect to a supersonic stream of hot air, which has a temperature $T_A = 1500$ K and pressure $p_A \sim 1.5$ bar. In fact, the temperature T_A is beyond the critical temperature above which a supercritical bifurcating response of the type shown in Figure 4(a) -in which no abrupt ignition or extinction occur- develops instead of the S-shaped curve of Figure 1(b) as predicted by Sánchez *et al.* (1996). The uncertainty bounds in the flamelet response of Figure 4(a) were calculated by using a Monte Carlo method with 200,000 flamelet solutions sampled from the reaction-rate stochastic space of the 20-step $H_2 - O_2$ mechanism of Hong *et al.* (2011) and by using method $\mathcal{M}_1$ for chemical-kinetic uncertainty modeling in Urzay *et al.* (2012), with the rates being subject to the uncertainty factors in Table 1 of Urzay *et al.* (2012). In particular, Figure 4(a) shows three different regions: i) An ignition or nearly-frozen region at high χ_{st} in which only pure mixing takes place, and which is subject to a very small chemical uncertainty; ii) a near-equilibirium region at small χ_{st}, in which the chemical time scales are so fast

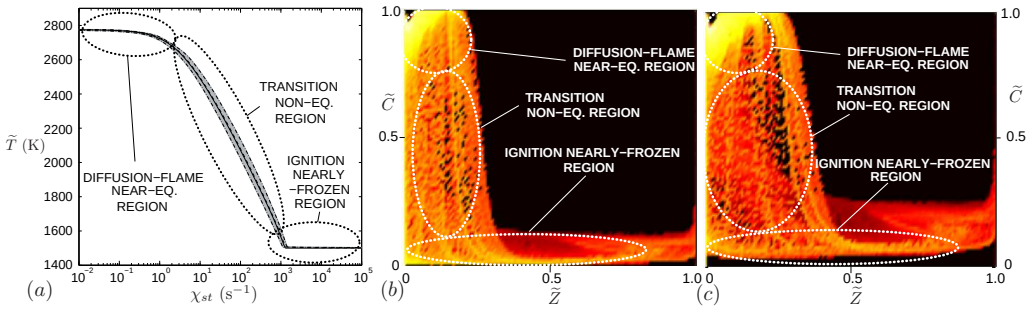

FIGURE 4. (a) Effects of chemical-kinetic uncertainties on the S-curve for HyShot-II flight conditions with grey area indicating ± 2 standard deviations, and logarithm of the joint PDF $P(\widetilde{Z},\widetilde{C})$ from deterministic RANS simulations for (b) non-diluted H_2-stream, and (c) 70% diluted H_2-stream with N_2 (same color scale from white -highest values- to black -lowest values).

compared to the diffusion time ℓ_m^2/D_{H_2} that the rate-constant uncertainties in Table 1 of Urzay *et al.* (2012) are not sufficient to cause any significant variations in the solution; and iii) a transition non-equilibrium region in which the chemical time scales are of the same order as the diffusion time ℓ_m^2/D_{H_2}, and in which the consideration of the uncertainties in the rates leads to $\Delta T_f = O(100\ \mathrm{K})$ temperature differences within the two standard-deviations bound. Note that these three regions were already predicted to occur in SCRAMJET engines in earlier work by Liñán *et al.* (1966).

In the HyShot-II the fast-chemistry zones occupy most of the combustor. This is revealed by the examination of the joint PDFs $P(\widetilde{Z},\widetilde{C})$ in Figure 4(b,c), where $\widetilde{C}$ has been scaled with the maximum value. By way of contrast, the presence of fuel dilution contributes to enlarge the transitional region, as observed in Figure 3(b) and Figure 4(c). Therefore, for the Hyshot-II SCRAMJET and in the FPVA-RANS framework, chemical-kinetic uncertainties lead to variations in the regions close to the injector, where finite-rate chemistry effects are important, and are mostly irrelevant downstream where fast chemistry occurs. The case of hydrogen combustion is also a pathological one, in that the rate constants of the $H_2 - O_2$ mechanism are extremely well characterized as opposed to the kinetics of heavy hydrocarbon fuels.

7. Conclusions

In this study, a method has been proposed to study, within the FPVA framework of turbulent-combustion modeling, the effects of high-dimensional chemical-kinetic uncertainties in partially-premixed high-speed turbulent combustion. The method employs two gates at the kinetics and flamelet levels in order to reduce the high-dimensional chemical uncertainties to a downsized stochastic space of flamelet variables.

Acknowledgments

This investigation was funded by the Predictive-Science Academic-Alliance Program (PSAAP), Grant # DE-FC52-08NA28614, for investigating uncertainties in hydrogen-fueled SCRAMJETS. The first author was supported by the 2011-2012 Postdoctoral Fellowship for Excellence in Research, Ibercaja Foundation (Zaragoza, Spain).

REFERENCES

Boivin, P., Jimenez, C., Sánchez, A. L. & Williams, F. A. 2011 An expected reduced mechanism for H_2-air combustion. *Proc. Comb. Inst.* **33**, 517–523.

Hong, Z., Davidson, D. F. & Hanson, R. K. 2011 An improved H_2/O_2 mechanism based on recent shock tube/laser absorption measurements. *Comb. Flame* **158**, 633–644.

Iaccarino, G., Sharp, D. & Glimm, J. 2012 Quantification of margins and uncertainties using multiple gates and conditional probabilities (To appear in *Reliab. Eng. Syst. Safety*) .

Liñán, A. 1974 The asymptotic structure of counterflow diffusion flames for large activation energies. *Acta Astronautica* **1**, 1007–1039.

Liñán, A., Urrutia, J. L. & Fraga, E. 1966 On diffusive supersonic combustion. *International Council of the Aeronautical Science Congress IV* pp. 607–618.

Mueller, M. E., Iaccarino, G. & Pitsch, H. 2012 Chemical kinetic uncertainty quantication for large eddy simulation of turbulent nonpremixed combustion. *Proc. Comb. Inst.* **34**, 1–8.

Najm, H. N., Debusschere, B. J., Marzouk, Y. M., Widmer, S. & Le Maitre, O. P. 2009 Uncertainty quantification in chemical systems. *Int. J. for Numer. Meth. Eng.* **80**, 789–814.

Pecnik, R., Terrapon, V. E., Ham, F., Iaccarino, G. & Pitsch, H. 2012 Reynolds-averaged Navier-Stokes simulations of the HyShot-II scramjet. *AIAA J.* **50** (8), 1717–1732.

Peters, N. 1983 Local quenching due to flame stretch and non-premixed turbulent combustion. *Combust. Sci. and Tech.* **30**, 1–17.

Peters, N. 2000 *Turbulent Combustion.* Cambridge University Press..

Pierce, C. D. & Moin, P. 2004 Progress-variable approach for large-eddy simulation of non-premixed turbulent combustion. *J. Fluid Mech.* **504**, 73–97.

Pitsch, H. & Peters, N. 1998 A consistent flamelet formulation for non-premixed combustion considering differential diffusion effects. *Comb. Flame* **114**, 26–40.

Sánchez, A. L., Balakrishnan, G., Liñán, A. & Williams, F. A. 1996 Relationships between bifurcation and numerical analyses for ignition of hydrogen-air diffusion flames. *Comb. Flame* **105**, 569–590.

Sánchez, A. L., Liñán, A., Williams, F. A. & Balakrishnan, G. 1995 Theory of structures of hydrogen-air diffusion flames. *Combust. Sci. and Tech.* **110**, 277–301.

Urzay, J., Kseib, N., Constantine, P., Davidson, D. F. & Iaccarino, G. 2012 Uncertainty-quantifying models for chemical-kinetic rates. *Annual Research Briefs*, Center for Turbulence Research, NASA Ames/Stanford University pp. 1–14.

Williams, F. A. 1985 *Combustion Theory.* Benjamin Cummings.